Advances in Natural and Technological Hazards Research
2014, Volume 37 Pages 129-139
http://dx.doi.org/10.1007/978-3-319-00972-8_12
http://archimer.ifremer.fr/doc/00226/33752/

Fluid Seepage in Relation to Seabed Deformation on the Central Nile Deep-Sea Fan, Part 1: Evidence from Sidescan Sonar Data

Dano Alexandre [1], Praeg Daniel [2], Migeon Sebastien [1], Augustin Jean-Marie [3], Ceramicola Silvia [2], Ketzer Joao Marcelo [4], Augustin Adolfo Herbert [4], Ducassou Emmanuelle [5], Mascle Jean [6]

[1] Géoazur, UMR7329, UNS-UPMC-CNRS-OCA, Rue Albert Einstein, 06560, Valbonne, France
[2] OGS (Istituto Nazionale di Oceanografia e di Geofisica Sperimentale), Borgo Grotta Gigante 42c, 34010, Trieste, Italy
[3] IFREMER, Technopôle Brest-Iroise, Plouzané, France
[4] Center of Excellence in Research and Innovation in Petroleum, Mineral Resources and Carbon Storage (CEPAC), Pontifical University of Rio Grande do Sul (PUCRS), Av. Ipiranga 6681, Prédio 96J, CEP 90619-900, Porto Alegre, RS, Brazil
[5] Université Bordeaux 1, UMR5805 EPOC, Avenue des facultés, 33405, Talence, France
[6] Géoazur, UMR7329, UNS-UPMC-CNRS-OCA, Porte de la Darse, Villefranche-sur-Mer, France

* Corresponding author : Alexandre Dano, email address : dano@geoazur.unice.fr

Abstract :

The central Nile Deep-Sea Fan contains a broad area of seabed destabilisation in association with fluid seepage: slope-parallel sediment undulations are associated with multibeam high-backscatter patches (HBPs) related to authigenic carbonates. During the 2011 APINIL campaign, a deep-towed sidescan and profiling system (SAR) was used to acquire high-resolution data along three transects across water depths of 1,700-2,650 m. Three seabed domains are distinguished, all developed within stratified sediments overlying mass-transport deposits (MTDs). Upslope of the undulations (<1,950 m), sidescan HBPs record focused fluid seepage via seabed cracks. In the western area of undulations, sidescan HBPs are distinct from intermediate-backscatter patches (IBPs) that extend up to 850 m parallel to the undulations, mainly along their downslope flanks; some contain sub-circular HBPs up to 300 m wide, three associated with smaller (<10 m) hydroacoustic gas flares. Focused fluid seeps are inferred to have shifted over time to form elongate carbonate pavements, preferentially along the footwalls of faults beneath the undulations that provide pathways for fluid flow. In contrast, in the eastern area of undulations, sidescan imagery reveal only slope-transverse furrows formed by turbulent flows, interpreted to indicate that fossil carbonates sampled during submersible operations have been exhumed by erosion.

Keywords : Fluid seepage, Sediment deformation, Backscatter, Gas flares

1 Introduction

Slope instabilities may be associated with features of seabed seepage (Lastras et al. 2004; Ramprasad et al. 2011), but it remains unclear whether fluid migration and release over time is a cause or consequence of sediment deformation. The Nile Deep-Sea Fan (NDSF) provides a useful study area, as investigations over the last decade have shown it to contain a rich variety of features of sediment destabilisation as well as of fluid migration and seepage (Loncke et al. 2004, 2009; Garziglia et al. 2008). The central NDSF contains a broad area of slope-parallel seabed undulations (Fig. 1), composed of stratified sediments overlying large mass transport deposits (MTDs), interpreted to record downslope deformation in association with fluid venting (Loncke et al. 2002, 2004; Bayon et al. 2009; Migeon et al. 2013). The undulations contain internal shear planes consistent with creeping and/or gliding of sediment blocks, while fluid seepage is recorded by patches of high acoustic backscatter up to 400m across corresponding to pockmarks and/or low mounds (Loncke et al. 2002, 2004). Submersible observations show the high-backscatter patches to coincide with authigenic carbonate pavements, and suggest a model in which downslope sediment deformation above a decollement at the top of the MTDs has created pathways for fluid seepage through the troughs of the undulations, while apparently causing fossil carbonates to be exhumed along their crests (Bayon et al. 2009). In contrast, submersible observations upslope from the undulations suggest that carbonate pavements record ongoing seepage by diffuse fluid flow through undeformed sediments overlying MTDs (Bayon et al. 2009).

New information on the central NDSF was acquired during the 2011 APINIL campaign, using high-resolution swath/profiling systems. These data provide evidence of a lateral change in character of the seabed undulations, interpreted to record the interaction of gravity-driven deformation with downslope depositional processes over time: younger structures recording ongoing deformation and fluid venting in the west, give way eastwards to older deformation structures that are being transformed into sediment waves (Migeon et al. 2013). Here we focus on results from deep-towed sidescan swaths (Fig. 1), which provide the highest resolution seabed imagery yet available from the central NDSF. We examine the variation in seabed character across the area, with particular interest in the relation of seabed seepage to sediment deformation.

2 Methods

Sidescan sonar imagery and 2-5kHz sub-bottom profiles were acquired using the deep-towed SAR (*Système Acoustique Remorqué*) developed by Ifremer, towed 80-100m above the seafloor at an average speed of 1ms^{-1} and positioned using a short-baseline acoustic system. The sidescan sonar insonified an 1100m wide

seabed swath with a spatial resolution of 0.25m across-track and 1m along-track, here gridded to 1.5m pixels. High frequencies (170/190 kHz) and low incidence angles mean that penetration is minimal and backscatter intensity is mainly controlled by seabed morphology and sediment type. The different data types, including water column gas flares, were visualised using Sonarscope software (Ifremer).

3 Results

Subottom profiles across the central NDSF in water depths of 1700-2650m (Fig. 1) show that the entire area is underlain by MTDs overlain by stratified sediments, both of which are thinner in depths <1950m (Figs 2, 3), here called the middle slope (cf. Bayon et al. 2009). Across the lower slope in depths >1950m, the stratified sediments are deformed into seabed undulations that thicken and change in character eastwards: in the west short, arcuate features correspond to rotated fault blocks, while in the east longer, linear features are interpreted as older deformation structures that are being progressively transformed into sediment waves (Migeon et al. 2013).

Four types of seabed feature were identified: 1) erosional furrows, 2) sediment cracks, 3) carbonate pavements and 3) hydroacoustic gas flares rising from seabed into the water column.

3.1 Erosional furrows

Seabed furrows consist of parallel lineaments 5-10m wide and up to 800m long, oriented transverse to slope (Fig. 3B). They are only observed along the eastern SAR transect (Fig. 1), from 2150-2500m water depth, oriented N-NW. They are located on the downslope flanks of the larger seabed undulations and on both upstream and downstream flanks of the smaller ones. They are interpreted to record erosion of the seabed by turbulent flows moving downslope, as part of the ongoing sedimentary accretion of undulations in this part of the slope (see Migeon et al. 2013).

3.2 Sediment cracks

Superficial sediment cracks are observed as radiating networks of lineaments of high backscatter (Figs 2A-B, 3A), up to 4m wide and 250m long. Cracks were observed along the western SAR transect (Fig. 1) in two different settings, on the middle and lower slope. On the middle slope, in water depths of 1690-1970m,

103 they are associated with a blocky seabed morphology developed above an acousti-
104 cally unstratified unit, together indicative of a mass transport deposit buried by
105 thin stratified sediments (Fig. 2A). The radiating cracks could result from compac-
106 tion following the emplacement of cohesive MTDs; some are associated with sea-
107 bed carbonates (Fig. 2A, see below) and could have either guided upward fluid
108 migration or been created by fluid flows. On the lower slope, they are seen on or
109 near the crests of stratified sediment undulations that have undergone rotational
110 tilting (Figs 2B, 3A). The cracks lie parallel to the crest undulations and are in-
111 ferred to be extensional structures related to fault block rotation.

112 *3.3 Carbonate pavements*

113 Carbonate pavements are inferred from sidescan backscatter anomalies of vary-
114 ing intensity, here referred to as high and intermediate backscatter patches (HBPs
115 and IBPs; Figs 2, 3A). On sidescan imagery, HBPs are up to 300m in diameter,
116 sub-circular to irregular in shape. They occur on the middle slope, on top of a
117 blocky mass flow, in association with seabed cracks (Fig. 2A). They also occur on
118 the lower slope, in the western area of seabed undulations, in association with
119 more extensive IBPs (Figs 2B, 3A), which exhibit lower but variable backscatter
120 intensities and are elongate parallel to the seabed undulations, with widths up to
121 200m and lengths up to 850m. The IBPs and HBPs are preferentially located along
122 the downslope flanks of the seabed undulations (Figs 2B, 3A), although they can
123 also extend across their troughs and crests. SAR 3.5kHz profiles show many
124 downslope flanks to be underlain by an incoherent acoustic facies consistent with
125 the presence of gas (Figs 2B, 3A). The HPBs and IBPs are interpreted as car-
126 bonate pavements formed in response to upward seepage of gas-rich fluids, as
127 shown by submersible observations elsewhere in the central NDSF (Bayon et al.
128 2009). They overlap with backscatter anomalies observed on lower frequency
129 multibeam data (Fig. 1) but are more extensive (see Praeg et al. 2013); however,
130 there are none along the lower part (water depths >1950m) of the eastern SAR
131 transect where no multibeam anomalies are observed (Fig.1).

132 *3.4 Hydroacoustic flares*

133 The SAR encountered gas flares in the water column at three sites, each near
134 HBPs observed on sidescan imagery. The flares are observed on data uncorrected
135 for slant-range, as vertical or slightly inclined features 3-10m wide and up to
136 100m high, i.e. the depth of the SAR above the seabed (Fig. 4). At each site a pair
137 of flares was observed, c.60m apart, recording separate bubble streams rising into
138 the water column. It was not possible to position the flares relative to the sidescan

swath, although they could be seen to lie to left or right of the SAR; in one case flares are seen to pass from one side to the other, indicating near-range features. Positioning of the flares using multibeam water column data (see Praeg et al. 2013) confirms that the flares lie at the edges of sidescan HBPs and indicates that features >250m from the SAR are not observed.

4 Discussion

Analysis of sidescan sonar data across the central NDSF allows the identification of three open-slope domains characterized by differing associations of sediment deformation and fluid seepage: a middle slope (depths <1950 m), and western and eastern areas of seabed undulations on the lower slope (depths >1950m).

4.1 Mid-slope domain: focused fluid flow through MTDs

The southern domain corresponds to the middle slope, in water depths of 1700-1950m, which is dominated by blocky MTDs 20-30m thick on average, draped by layered deposits up to 2m thick (Fig. 2A). From sedimentation rates estimated from cores in the area (Ducassou et al. 2009), the MTDs could be at least 10kyrs old. Isolated HBPs observed above the MTDs in association with seabed cracks (Fig. 2A) indicate authigenic carbonate pavements formed from seepage of gas-rich fluids, unlikely to have come from dewatering of the relatively thin MTDs following their emplacement. Gas-rich fluids suggest focused fluid flow from depth, which exploited pathways offered by the cracks. This is in contrast to results from submersible observations on the slope to the east, in water depths of 1650m, where seabed carbonate pavements above MTDs were shown to record downward growth over the last 5kyrs and suggested to record diffuse fluid flow (Bayon et al. 2009b). The broad carbonate pavements (incuding IBPs up to 1.4 km across) are more likely to record growth over time by lateral displacement of sites of focused seepage, as suggested by Dupré et al. (2010).

4.2 Western undulations: fluid flow along faults rooted in MTDs

The western domain of seabed undulations contains abundant backscatter patches of high to intermediate intensity (Figs 2, 3A), indicative of carbonate formation in response to the migration and seepage of gas-rich fluids (cf. Bayon et al. 2009). The carbonate pavements are oriented sub-parallel to the seabed undulations, which record gravity-driven deformation of the upper sediment cover, in an

area where the mean slope angle is 2.5° (Migeon et al. 2013). As gas charging is known to decrease sediment shear strength through time, which can contribute to creeping and/or landsliding processes (Locat and Lee 2002), fluid circulation is inferred to play a key role in the development of shallow instabilities on the central NDSF. In turn, our results provide evidence that sediment deformation has influenced fluid circulation.

Results from SAR sidescan imagery in the west of the study area indicate a distinction between sub-circular HBPs up to 300m across, several of which are associated with smaller (<60m) sites of gas venting, and broader areas of intermediate backscatter (IBPs) that extend up to 850m along the seabed undulations. Backscatter patches of varying intensity have also been observed on 75kHz sidescan sonar imagery from the central NDSF, upslope of the seabed undulations, which showed areas of variable (intermediate) backscatter up to 1400m across, within which occur smaller HBPs, some with gas flares at their edges (Dupré et al. 2010). The authors suggested that blocking of fluid flow by carbonate growth leads to lateral displacement of sites of seepage and the formation over time of broad carbonate sheets. Our results are consistent with this mechanism, which we apply to explain variable backscatter intensities in terms of successive stages of carbonate formation: IBPs correspond to fossil seepage sites, which may be covered by a thin veneer of sediment, while HBPs correspond to exposed areas of carbonates, within which backscatter may be enhanced both by micro-relief and by bioactivity related to active gas seepage (Dupré et al. 2010).

The SAR imagery shows that, in the western part of the study area, the growth over time of carbonate pavements is taking place along elongate zones, parallel to the seabed undulations. The formation of carbonate pavements appears to be favoured along the downslope facing flanks of the undulations, above faults assumed to bound rotated sediment blocks (Fig. 3A; Migeon et al. 2013). We infer that the faults act as fluid migration pathways, leading to preferential formation of carbonates along their footwalls.

4.3 Eastern undulations: exhumation of fossil carbonates

In the eastern domain of seabed undulations, neither IBPs nor HBPs were observed on sidescan imagery, consistent with the eastward decrease in density of HBPs observed on multibeam data (Fig. 1; Migeon et al. 2013). A reduced fluid flux is supported by submersible observations in an aarea 2km east of the SAR transect (Fig. 1), which found dissolved methane anomalies in the troughs of some undulations but did not encounter gas bubbles (Bayon et al. 2009). The same study showed carbonate pavements on the crest of one undulation to be fossil features, dated at c. 8kyrs, suggested to have been exhumed by deformation associated with formation of the seabed undulations. Our results suggest instead that these carbonates have been exposed by seabed erosion associated with the formation of

elongated furrows, recording downslope particle transport by gravity flows (Fig. 3B). The predominance of sediment transport and deposition in the eastern domain, and the reduced importance of fluid circulation and gas venting, is consistent with an interpretation of the seabed undulations as older deformation structures that are being transformed into sediment waves (Migeon et al. 2013). Sedimentation could also contribute to the burial of seeps on the upslope flanks of undulations, a further explanation for their limited observation.

5 Conclusions

Changes in seabed character across the central NDSF observed on sidescan sonar imagery distinguish three main slope associations of sediment deformation and fluid seepage. A mid-slope (<1950m) area contains evidence of focused fluid flow from depth that has exploited seabed cracks developed above recent mass failure deposits. On the lower slope (>1950m), a broad area of seabed undulations changes in character from west to east. In the west, abundant evidence of seabed seepage correlates with shallow faults recording ongoing sediment deformation, which are inferred to have provided pathways for active seeps that have shifted over time to form broad carbonate pavements elongate along the seabed undulations. In the east, decreased evidence of seepage activity correlates with an increase in sediment furrows recording erosion by turbulent flows, which is inferred to have exhumed fossil carbonates sampled during submersible observations.

Acknowledgements The authors thank the captain and crew of the RV Le Suroît and their colleagues at sea and ashore who supported the APINIL campaign. This work was funded by CNRS-INSU and the French programme Action Marges. The manuscript was improved by helpful reviews from Renato Kowsmann (Petrobras, Rio di Janeiro) and Dave Long (BGS, Edinburgh).

References

Bayon G, Loncke L, Dupré S, Caprais J-C, Ducassou E, Duperron S, Etoubleau J, Foucher J-P, Fouquet Y, Gontharet S, Henderson GM, Huguen C, Klaucke I, Mascle J, Migeon S, Ondréas H, Pierre C, Sibuet M, Stadnitskaia A, Woodside J (2009) Multi-disciplinary investigation of fluid seepage on an unstable margin: The case of the Centre Nile deep sea fan. Mar Geol 26:92-104.

Ducassou E, Migeon S, Mulder T, Murat A, Capotondi L, Bernasconi SM, Mascle J (2009) Evolution of the Nile deep-sea turbidite system during the Late Quaternary : influence of climate change on fan sedimentation. Sedimentology 56:2061-2090.

Dupré S, Woodside J. Klaucke I, Mascle J, Foucher J-P (2010) Widespread active seepage activity on the Nile deep Sea Fan (offshore Egypt) revealed by high-definition geophysical imagery. Mar Geol 275:1-19.

Garziglia S, Migeon S, Ducassou E, Loncke L, Mascle J (2008) Mass-transport deposits on the Rosetta province (NW Nile Dea-sea turbidite system, Egyptian margin): characteristics, distribution, and potential causal processes. Mar Geol 250:180-198.

Lastras G, Canals M, Urgeles R, Hughes-Clarke JE, Acosta J (2004) Shallow slides and pockmarks swarms in the Eivissa Channel, western Mediterranean Sea. Sedimentology 51:837-850.

Locat J, Lee HJ (2002) Submarine landslides: advances and challenges. Can Geotech J 39:193-212.

Loncke L, Gaullier V, Droz L, Ducassou E, Migeon S, Mascle J (2009) Multi-scale slope instabilities along the Nile deep-sea fan, Egyptian margin: A general overview. Mar Petr Geol 26:633-646.

Loncke L, Mascle J, Fanil Scientific Parties (2004) Mud volcanoes, gas chimney, pockmarks and mounds in the Nile deep-sea fan (Eastern Mediterranean): geophysical evidences. Mar Pet Geol 21:669-689.

Migeon S, Ceramicola S, Praeg D, Ducassou E, Dano A, Ketzer JM, Mascle J (2013) Post-failure processes on the continental slope of the Central Nile Deep-Sea Fan: interactions between fluid seepage, creeping and sediment wave construction. In: Submarine Mass Movements and Their Consequences,6th International Symposium; Springer (this volume).

Praeg D, Ketzer JM, Augustin AH, Migeon S, Augustin J-M, Ceramicola S, Dano A, Ducassou E, Dupré S, Mascle J, Rodrigues LF (2013) Fluid seepage in relation to seafloor deformation on the central Nile Deep-Sea Fan, part 2: evidence from multibeam and sidescan imagery. In: Submarine Mass Movements and Their Consequences, 6th International Symposium. Springer (this volume)

Ramprasad T, Dewangan P, Ramana MV, Mazumdar A, Karisiddaiah SM, Ramya ER, Sriram G (2011) Evidence of slumping/sliding in Krishna-Godavari offshore basin due to gas/fluid movements. Mar Petr Geol 28 :1806-1816.

Rouillard P (2010) Modèles architectural et lithologique des dépôts quaternaires du système de Rosetta (Delta Profond du Nil, Méditerranée orientale) : implication pour un analogue actuel de réservoirs pétroliers. PhD Thesis, University of Nice-Sophia Antipolis, 421 pp.

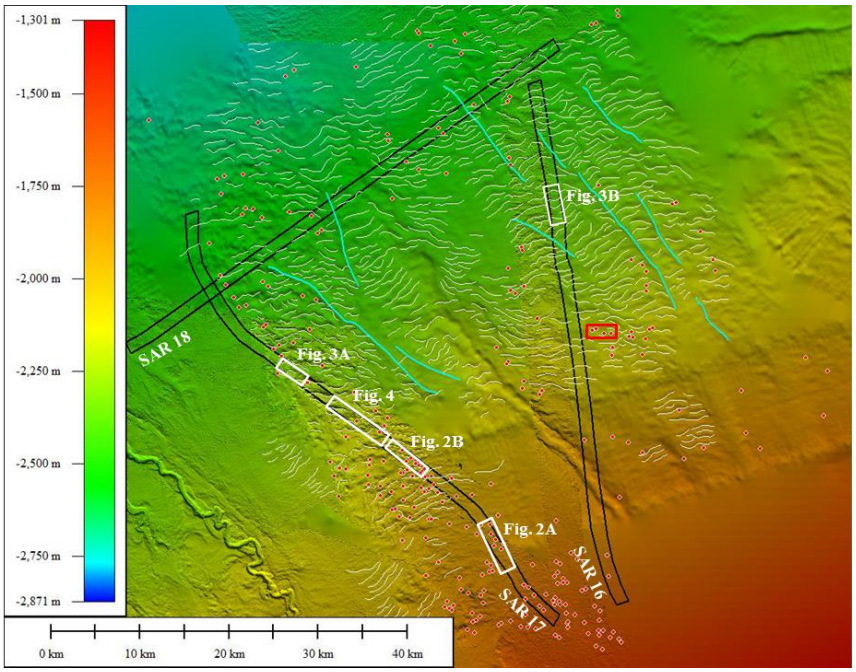

Fig. 1: Bathymetric map of the study area in the central NDSF. Red dots are multibeam high-backscatter patches. White continuous lines display crests of seabed undulations. Blue lines are small sediment pathways. The red square locates submersible investigations of carbonate pavements (Bayon et al., 2009).

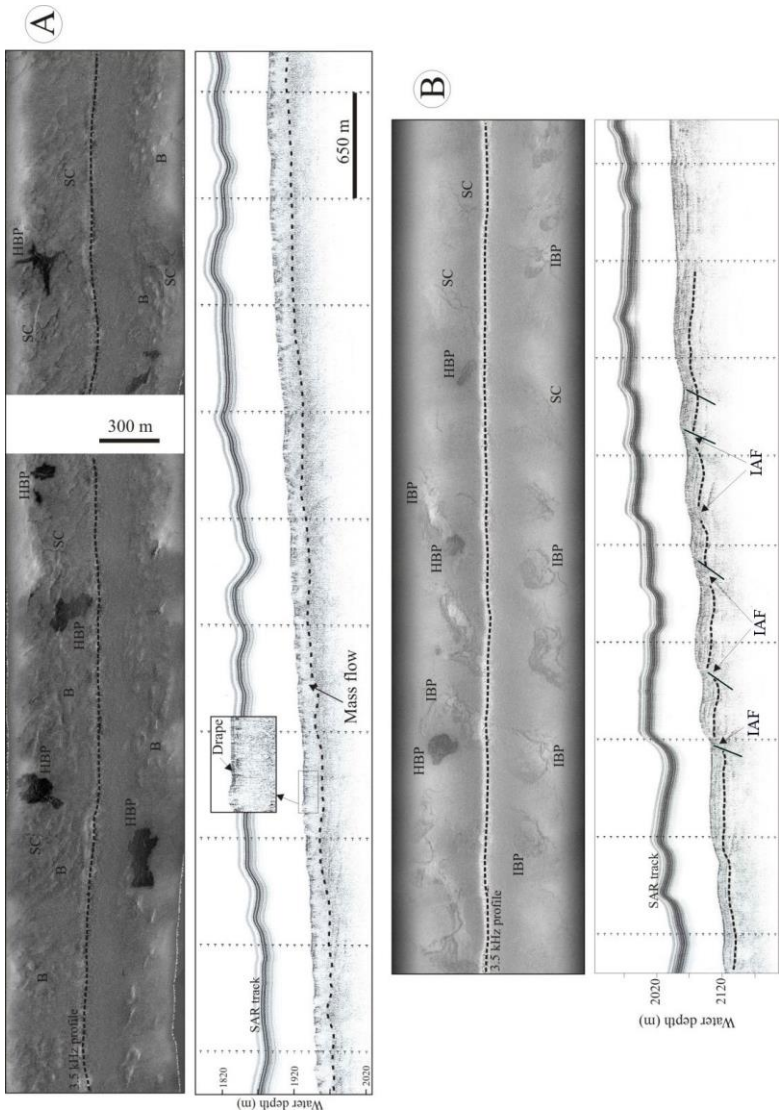

Fig. 2: SAR sidescan imagery (upper) and 3.5 kHz sub-bottom profiles (lower): A) middle slope, across a mass-flow deposit with blocks (B), high-backscatter patches (HBP) and sediment cracks (SC); B) lower slope, across sediment undulations associated with HBPs and intermediate-backscatter patches (IBP), as well as sediment cracks (SC); the IBPs (and cracks) are oriented parallel to the undulations and correlate at depth with incoherent acoustic facies (IAF) interpreted as gas-rich signatures along faults bounding the deformation structures. Locations in Figure 1.

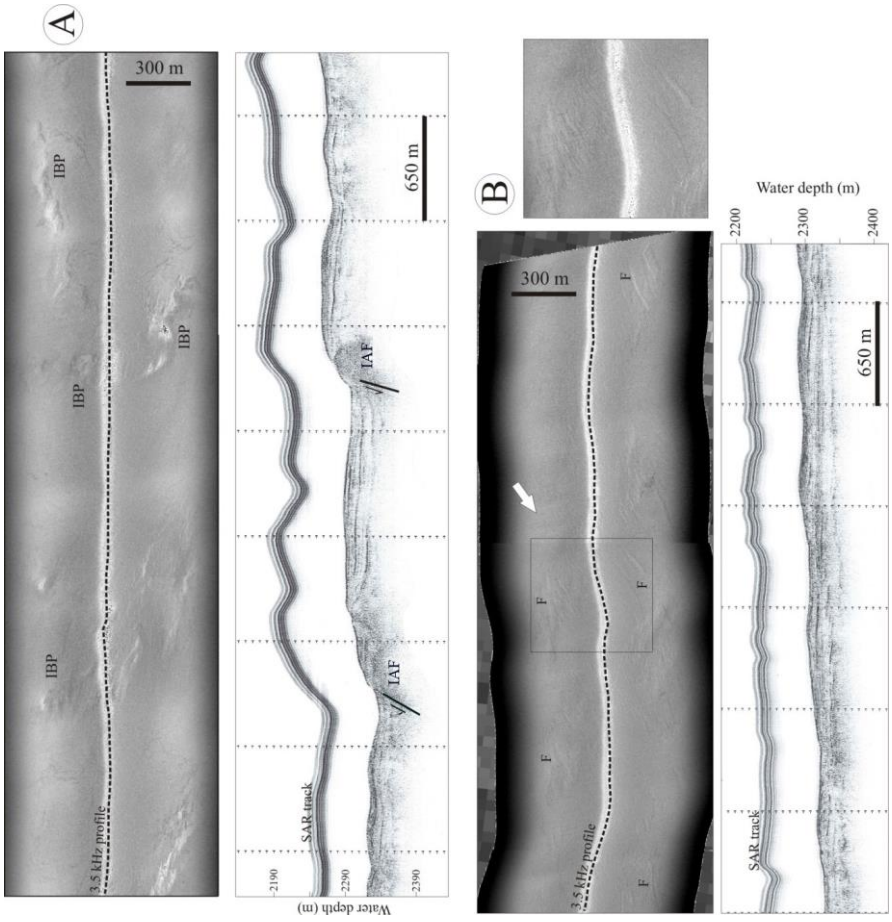

Fig. 3: SAR sidescan imagery (upper) and 3.5 kHz profiles (lower): A) across sediment undulations associated with intermediate-backscatter patches (IBP) located along the footwalls of faults seen at depth and correlated with incoherent acoustic facies (IAF) indicative of gas; B) across sediment undulations affected by downslope-oriented furrows (F) related to recent turbulent flows. The white arrow indicates the main direction of flows. Locations shown in Figure 1.

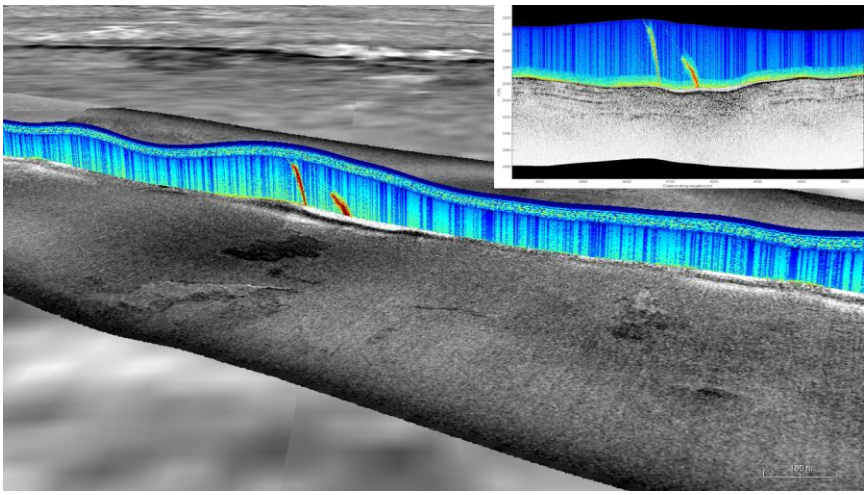

Fig. 4: Identification of gas flares in the SAR water column data. The flares are 3-10 m wide and c. 60 m apart, inferred to lie within 250 m of the high-backscatter patch observed at seabed (the swath is 1100 m wide on figure, 550 m on each side). Inset: correlation of gas flares to gas signatures (IAF) on 2-5kHz sub-bottom profile.